ENVIRONMENTAL RESEARCH
LETTERS

LETTER • OPEN ACCESS

Temporal connections between extreme precipitation and humid heat

To cite this article: Sophie Johnson *et al* 2024 *Environ. Res. Lett.* **19** 114076

ENVIRONMENTAL RESEARCH
LETTERS

OPEN ACCESS

RECEIVED
10 January 2024

REVISED
16 August 2024

ACCEPTED FOR PUBLICATION
24 September 2024

PUBLISHED
17 October 2024

LETTER

Temporal connections between extreme precipitation and humid heat

Sophie Johnson[1,3], **Catherine Ivanovich**[2], **Radley M Horton**[2,3,*], **Mingfang Ting**[2,3], **Kai Kornhuber**[2,4] and **Corey Lesk**[5]

[1] ICF International Inc., Reston, VA, United States of America
[2] Lamont-Doherty Earth Observatory, Columbia University, Palisades, NY, United States of America
[3] Columbia Climate School, Columbia University, New York City, NY, United States of America
[4] International Institute for Applied Systems Analysis (IIASA), Laxenburg, Austria
[5] Neukom Institute and Department of Geography, Dartmouth College, Hanover, NH, United States of America
[*] Authors to whom any correspondence should be addressed.

E-mail: rh142@columbia.edu

Keywords: extreme precipitation, humid heat, compound extremes, sequential extremes

Supplementary material for this article is available online

Abstract

Individually, extreme humid heat and extreme precipitation events can trigger widespread socioeconomic impacts which disproportionately affect vulnerable populations. These impacts might become greater when both events occur in close temporal proximity, for example if emergency responses to heat stress casualties are hindered by flooded roads. Improved understanding of the probabilities and physical mechanisms associated with these events' temporal compounding might uncover causal interrelationships offering avenues for improving early warning systems and projecting changes in a warmer climate. We explore sequential humid heat and rainfall relationships during the local summer season, identifying two classes of temporal relationships. We find that high wet bulb temperature (WBT) anomalies in most mid- to high-latitude and tropical regions are preceded by anomalously low precipitation. In contrast, hot and dry subtropical regions generally experience elevated WBTs during and, to a somewhat lesser extent, before extreme precipitation events. High WBT events are followed by positive precipitation anomalies in many land regions.

1. Introduction

Heat events are among the most deadly and damaging types of climate extremes (Horton *et al* 2016). Humid heat extremes are a health danger disproportionately affecting the most vulnerable populations, including those with pre-existing health conditions, the elderly, infants, and those without access to protective infrastructure and services such as air conditioning (Romanello *et al* 2022, Diaz *et al* 2023). Heat becomes particularly harmful to human health when combined with high humidity, as high humidity hinders the body's ability to cool itself through sweating (Sherwood and Huber 2010). Extreme precipitation events are likewise a hazard associated with direct loss of life due to flash flooding, but also with damage to infrastructure and agriculture, which is often concentrated in low-lying flood plains alongside vulnerable populations (Caretta *et al* 2022) and urban areas (Hemmati *et al* 2022). However, combinations of humid heat and precipitation are an emerging and often underappreciated hazard in many regions around the world.

Globally, the frequency and intensity of both humid heat events and extreme precipitation have been increasing (Robinson *et al* 2021), and are projected to increase further in the future (IPCC 2021). Raymond *et al* (2020) report a doubling of extreme humid heat events globally over the past 40 years, and populations exposed to humid heat have increased faster than those exposed to high temperatures alone (Rogers *et al* 2021). Coffel *et al* (2017) project more than tenfold increases globally in humid heat by late in the 21st century under RCP 8.5, with even more

rapid increases in human exposure. Extreme precipitation trends have likewise been strongly positive across much of the globe (Sun *et al* 2021). As one example, relative to a 1901–1960 base period, in the relatively data-rich contiguous U.S., the frequency of 2-day extreme precipitation events has increased by approximately 40% in the last two decades (Easterling *et al* 2017). The coarse resolution of global climate models and other challenges make it more difficult to project extreme precipitation changes than other variables like temperature. However, diverse methodologies (e.g. Prein *et al* 2017, Lenderink and Attema 2015) strongly support the idea that as a global average the frequency and intensity of extreme precipitation should increase, potentially at rates that far exceed changes in mean precipitation (Zhang *et al* 2017), leading to large increases in population exposed (Chen and Sun 2021).

This concomitant increase in humid heat and extreme precipitation increases the likelihood of both occurring in close temporal proximity (Raymond *et al* 2022). A growing body of research is thus exploring compound extreme events (Zscheischler *et al* 2020) and their impacts (Raymond *et al* 2020). Such combinations can cause non-linear compounding impacts: extreme rainfall and ensuing flooding may compromise energy and transportation infrastructure, removing access to air conditioning or the opportunity for departing to a safer location as humid heat arrives. Humid heat may also stress emergency workers responding to extreme rainfall impacts, slowing recovery and impeding rescue. A key point is that multivariate impacts can occur even if one of the two variables is not in an extreme state (Raymond *et al* 2020, Zscheischler *et al* 2020). While such sequences can be expected due to chance alone, the potential for non-linear *excess* impacts when sequential events occur, points to the need for research on their statistical and physical relationships: when, where, and why are positive or negative correlations between the two types of extremes to be expected? Humid heat–all other conditions being equal–is associated with high convective available potential energy (Raymond *et al* 2021), and thus could potentially lead to heavy rainfall, if not inhibited by other factors like large-scale subsidence. Conversely, in moisture limited environments, anomalous precipitation itself across a range of timescales might thereafter offer a source of atmospheric humidity through surface evaporation, thus supporting humid heat (Kong and Huber 2023, Ivanovich *et al* 2024).

Recent studies have explored relationships between humid heat and rainfall or flooding, generally (1) centering on precipitation and flooding and exploring humid heat as a cause, and/or (2) focusing on a single country. Chen *et al* (2021) showed that consecutive flood and heat events have been increasing in China over the past decades, while Zhang and Villarini (2020) highlighted the role of humid heat stress in flooding events over the US. Ali *et al* (2018) provided evidence for a contribution of dew point temperatures to precipitation extremes from a global perspective, and Wu and Wang (2021) focused a similar analysis on the U.S. Matthews *et al* (2019) showed that creeping changes in mean temperatures alone would lead to more sequences of coastal flooding associated with tropical cyclones, followed by humid heat extremes. To our knowledge, ours is the first study to apply a global lens to sequential humid heat and rainfall relationships, while devoting as much attention to humid heat in its own right as to rainfall. Understanding the temporal relationship between humid heat and precipitation is critical for better understanding the drivers behind sequential events and for improving community resilience in a warmer world.

2. Data & methods

Global hourly 2-m temperature, 2-m dewpoint temperature, and precipitation data was retrieved from the fifth major global reanalysis produced by the European Centre for Medium-Range Weather Forecasts (ERA5) high-resolution product (Hersbach *et al* 2020) (1979–2019). These hourly datasets were then converted to daily mean and daily maximum temperature, daily mean specific humidity, and daily total precipitation, then regridded to a $1^\circ \times 1^\circ$ grid due to computational constraints. All analyses were conducted during the local summer season, defined as June–August (JJA) for the Northern Hemisphere and December–February (DJF) for the Southern Hemisphere. Daily maximum wet bulb temperatures (WBT) were calculated separately, as in Rogers *et al* (2021), using code adapted from Kopp (2020), that executes an algorithm from Buzan *et al* (2015) for the Davies-Jones (2008). Of note, this calculation includes other variables not analyzed here but used for the background calculations of WBT including surface pressure.

Daily summer climatologies were calculated at each gridpoint for precipitation and WBT and smoothed with a 30-day running mean. Use of a 30-day running mean smoothes the day-to-day climatology by removing the random timing of stochastic weather events, such as rare tropical cyclones in the Southwest U.S. (experimentation with shorter smoothing windows of 5 and 10 days had negligible impacts on the results). Daily anomalies were computed by subtracting these smoothed climatologies from the raw daily data. Extreme WBT values were computed using the 90th percentile threshold of the daily anomalies. In contrast, the 90th percentile precipitation threshold is calculated using only the subset of days that include at least 1 mm of rainfall (experimentation with different percentiles had negligible

impacts on results, as can be seen in supplemental figures S10 and S11). Anomalies were used to remove the predominating influence of the seasonal cycle on humidity, temperature, and precipitation, which would obscure the influence of synoptic variability. Relatedly, anomalies better capture relatively extreme events outside the warmest or the wettest weeks in the seasonal composites.

The daily average WBT anomalies conditioned on extreme precipitation anomaly days, relative to WBT anomalies on all days of the summer months, were composited to generate global maps in the days prior to and following an extreme precipitation anomaly day. Single days prior to and after extreme event days were computed, as shown in the supplemental figures S6 and S7, but composite maps showing the average of the 3 days before and the 3 days after an extreme event are shown in figures 1 and 2 to offer a digestible snapshot of gridded results across the entire globe that summarizes the conditions immediately preceding and following each extreme event. We compute these composite maps for (a) the single day of the local extreme precipitation event, and the average across 3 days (b) before and (c) after the local extreme precipitation event. These global composites were also generated in the reverse direction, plotting precipitation anomalies conditioned on local extreme WBT events. The methods used for these two sets of composites were repeated using dry bulb temperature (DBT) in place of WBT for comparison. Lastly, a two-sample Kolmogorov–Smirnov test for goodness of fit was conducted and grid cells with a p-value of less than 0.05 were plotted on top of each global difference map to show areas of significance.

In addition to the gridpoint-level analysis, three climatologically-distinct case study regions were selected post-hoc in order to explore the temporal evolution of conditions during extreme events in regions showing strong signals (see figure 3). The regions analyzed include (1) 'subtropical dry' in southernmost Arizona/California (SAC), (2) 'mid- to high-latitude' in the region 'East of James Bay' (EJB), and (3) 'tropical wet' in Western Bangladesh/Eastern India (WBEI). SAC features a subtropical dry monsoonal climate and covers 32.5–37.5° N and 243.5–248.5° E; EJB has a temperate-cool to subarctic climate characterized by large temperature variability and progression of fronts, and covers 49.5–55.5° N and 282.5–289.5° E; and WBEI typifies a tropical/subtropical very wet monsoonal climate and covers 22.5–24.5° N and 87.5–90.5° E (see the blue boxes in figure 1(b)). In each of these regions, we show the evolution of WBT, specific humidity, DBT, and precipitation over the eleven days surrounding a 90th percentile precipitation event. A broader range of days was shown for this regional analysis to more fully capture the temporal evolution of different variables surrounding extreme events defined for the region as a whole (as opposed to at the gridbox level). Summer daily total precipitation, maximum WBT, mean DBT and mean specific humidity data from ERA5 were averaged across all grid points for the three regions, after the locations were selected from the raw daily data. The daily anomalies for these region averages were then calculated as above. Composites showing the temporal evolution of these variables five days before and after extreme precipitation events were then plotted for each region described above.

3. Results

On the day of the extreme precipitation event (Day 0, figure 1(b)), strong positive WBT anomalies tend to be present over relatively dry subtropical regions such as southwestern North America, the Sahel, parts of Tibet, southwest Africa, and much of Australia. Positive anomalies are also observed in mid/high latitude northeastern North America. Negative anomalies of generally lower magnitudes are observed over much of the tropical land masses, and parts of northern hemisphere mid-latitude regions such as northwestern North America, and much of Mediterranean Europe. These negative anomalies are also prevalent over much of Southeast Asia. Traces of these Day 0 anomaly patterns can be observed predominantly over land regions in the three preceding days (figure 1(a)) as WBT anomalies progressively build leading up to the extreme precipitation event, with this signal often significant over land regions (supplemental figure S7). However, perhaps the most striking phenomenon is the marked shift to anomalously low WBTs across almost the entire mid- and high-latitude land masses of the northern hemisphere—with the exception of those aforementioned subtropical areas with the strongest positive WBT anomalies—on the three days after extreme precipitation events (figure 1(c)). These negative anomalies attenuate over the next two days, but at a slightly lesser rate than the pre-extreme-rain event WBT anomalies grow (supplemental figure S7). Unlike the heterogeneous mixture of positive and negative WBT anomalies across the globe on 90th percentile precipitation days, DBT anomalies over land on those same locally high precipitation days are almost universally cooler than normal (figure 1(d)).

Figure 2's methodology is identical to figure 1, except here precipitation is conditioned on 90th percentile humid (panels (a)–(c)) and dry heat events (panel (d))—the reverse of the analysis shown in figure 1. Consistent with patterns identified in figure 1, large negative precipitation anomalies occupy much of the tropical and subtropical land masses on the day of extreme humid heat events. The meridional extent of these negative precipitation

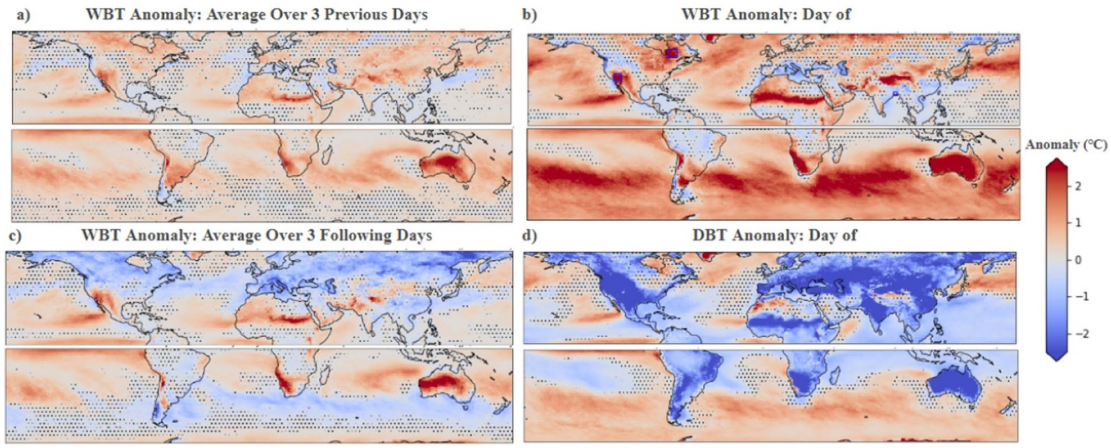

Figure 1. Composite maps of daily mean WBT and DBT anomalies conditioned on the 3 days before, the day of, and the 3 days after extreme 90th percentile precipitation days versus all days for local summer months (JJA for Northern Hemisphere; DJF for Southern Hemisphere). Stippling represents the two-sample Kolmogorov–Smirnov test for goodness of fit with a *p*-value of less than 0.05 to show areas of significance at the 90th percentile, with stippling showing areas that are not significant. Local WBT anomalies (a) averaged across 3 days prior to an extreme precipitation day, (b) conditioned on extreme precipitation days, and (c) averaged across 3 days after an extreme precipitation day. (d) Local DBT anomalies conditioned on extreme precipitation days.

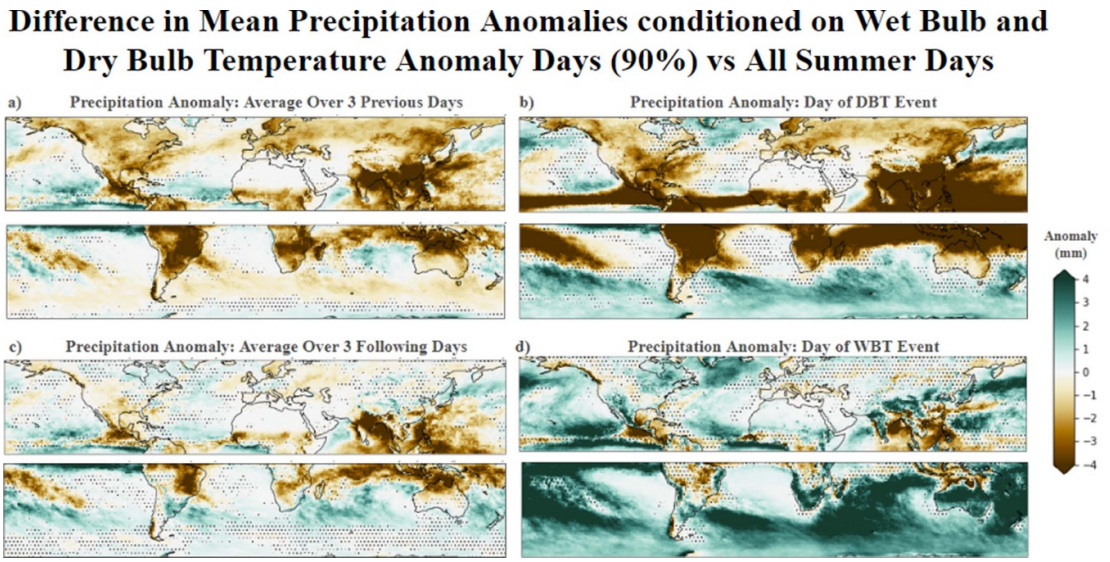

Figure 2. Composite maps of daily mean precipitation anomalies conditioned on the 3 days before, the day of, and the 3 days after extreme 90th percentile WBT and DBT days versus all days in local summer months (JJA for Northern Hemisphere; DJF for Southern Hemisphere). Stippling represents the two-sample Kolmogorov–Smirnov test for goodness of fit with a *p*-value of less than 0.05 to show areas of significance at the 90th percentile, with stippling showing areas that are not significant. Local precipitation anomalies (a) averaged across 3 days prior to an extreme WBT day, (b) conditioned on extreme WBT days, and (c) averaged across 3 days after an extreme WBT day.(d) Local precipitation anomalies conditioned on extreme DBT days.

anomalies is smallest over Africa, and largest over Eastern Asia, where it extends into the mid-latitudes. It should be noted though that while these negative anomalies exist over land, they are most prominent over water bodies relatively near the coast, such as the Bay of Bengal, the South China Sea, and the seas north of Australia; more generally, regions with large climatological rainfall in the summer season have potential for the greatest magnitude of negative precipitation anomalies. As might be expected given the inversion of the conditioning between figures 1 and 2, many of the spatial patterns observed in figure 1 for WBT (like anomalously high WBTs on the days leading up to 90th percentile precipitation events) manifest in figure 2 as anomalously high precipitation after 90th percentile wet bulb events. However, one region where the spatial pattern is not mirrored between figures 1 and 2 is the Sahel. WBT is elevated during extreme precipitation events, but WBTs can also be anomalously high without extreme precipitation, potentially due to the unique rainfall patterns in the region.

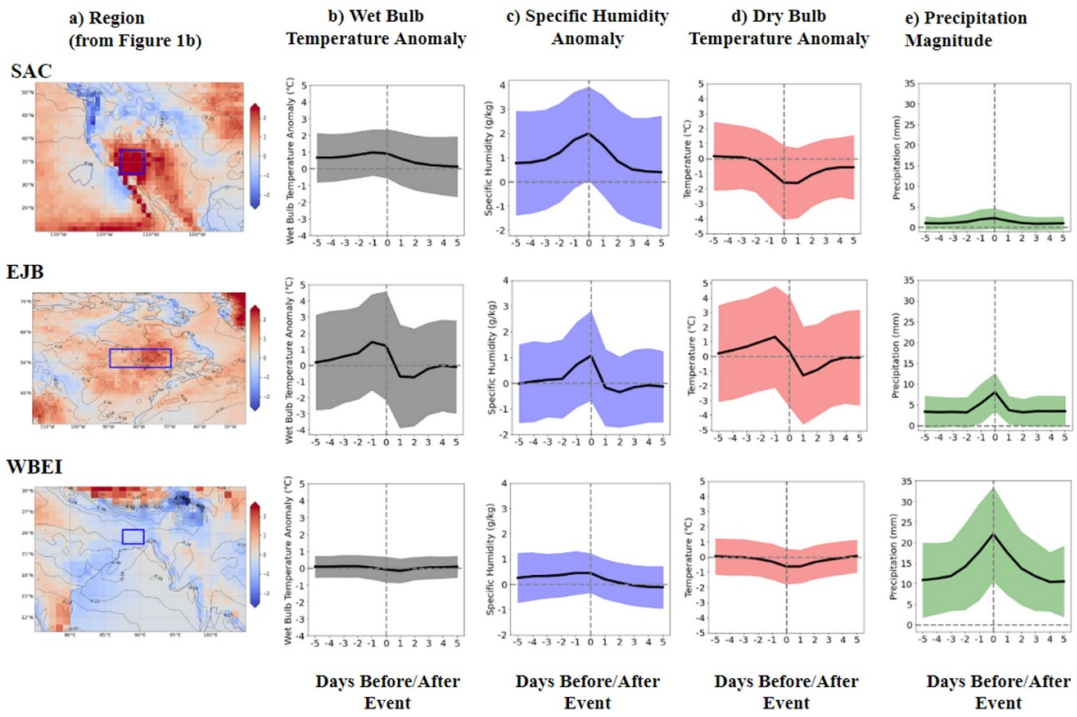

Figure 3. Regionally-averaged wet bulb temperature, specific humidity, dry bulb temperature, and precipitation anomalies in the 5 d before and after extreme precipitation events in the predefined SAC, EJB, and WBEI regions. Regional boundary boxes overlaid on figure 1(b) are shown in the first panel on the left. Colored shading in each plot shows ±1 standard deviation.

Whereas figures 1(b) and 2(b) relate WBT to same-day precipitation, the figures 1(d) and 2(d) contrast DBT to precipitation. The tendency for anomalously low land precipitation when conditioned on high DBT is very pronounced across almost all land areas, with the largest exception being a portion of northwest Africa. These near-universal negative associations between DBT and precipitation are presumably due to factors including more sunlight and subsidence on high DBT days, and less evaporative cooling in the absence of rain events.

We find that the evolution of composite humidity and temperatures preceding and following extreme precipitation differs importantly across regions (figure 3; see supplemental figure S8 and associated text for regional analysis of extreme WBT days). WBEI tends to experience WBT suppression on heavy rain days, with relatively large reduction of DBTs outweighing a slight increase in specific humidity. The slight suppression of WBT on heavy precipitation days is prevalent across eastern portions of South Asia. SAC shows an opposite pattern between precipitation and humid heat, with heavy rains associated with elevated WBT. Here, large increases in specific humidity outweigh smaller decreases in DBT. Both regions also feature moderately elevated specific humidity in the days leading up to the heavy rain event, with positive humidity anomalies and negative DBT anomalies gradually disappearing post-event. The EJB region, like SAC, features positive WBT anomalies on the day of and the day before extreme precipitation. However, unlike in the other two regions, here positive anomalies of both specific humidity and DBT co-occur, likely associated with extreme rainfall occurring in the warm sector of midlatitude cyclones, right along the advancing cold front. SAC exhibits a similar pattern to WBEI, with negative DBT anomalies on the day of extreme precipitation which slowly increase in the days after, but positive specific humidity anomalies on the day of extreme precipitation which drop sharply in the days after. The relationship between precipitation amounts and soil moisture evolution differs across regions, likely mediated by complexities of regional hydrology. Soil moisture (supplemental figure S9, column f) increases in all three regions during and after the extreme precipitation days, with positive anomalies persisting until the end of the 5 day post-event period. In the days leading up to the heavy rain event, the SAC region (and to a lesser extent, the WBEI region) show small positive soil moisture anomalies.

Figure 4 shows the full distribution for the secondary variable, rather than solely the mean, on 90th

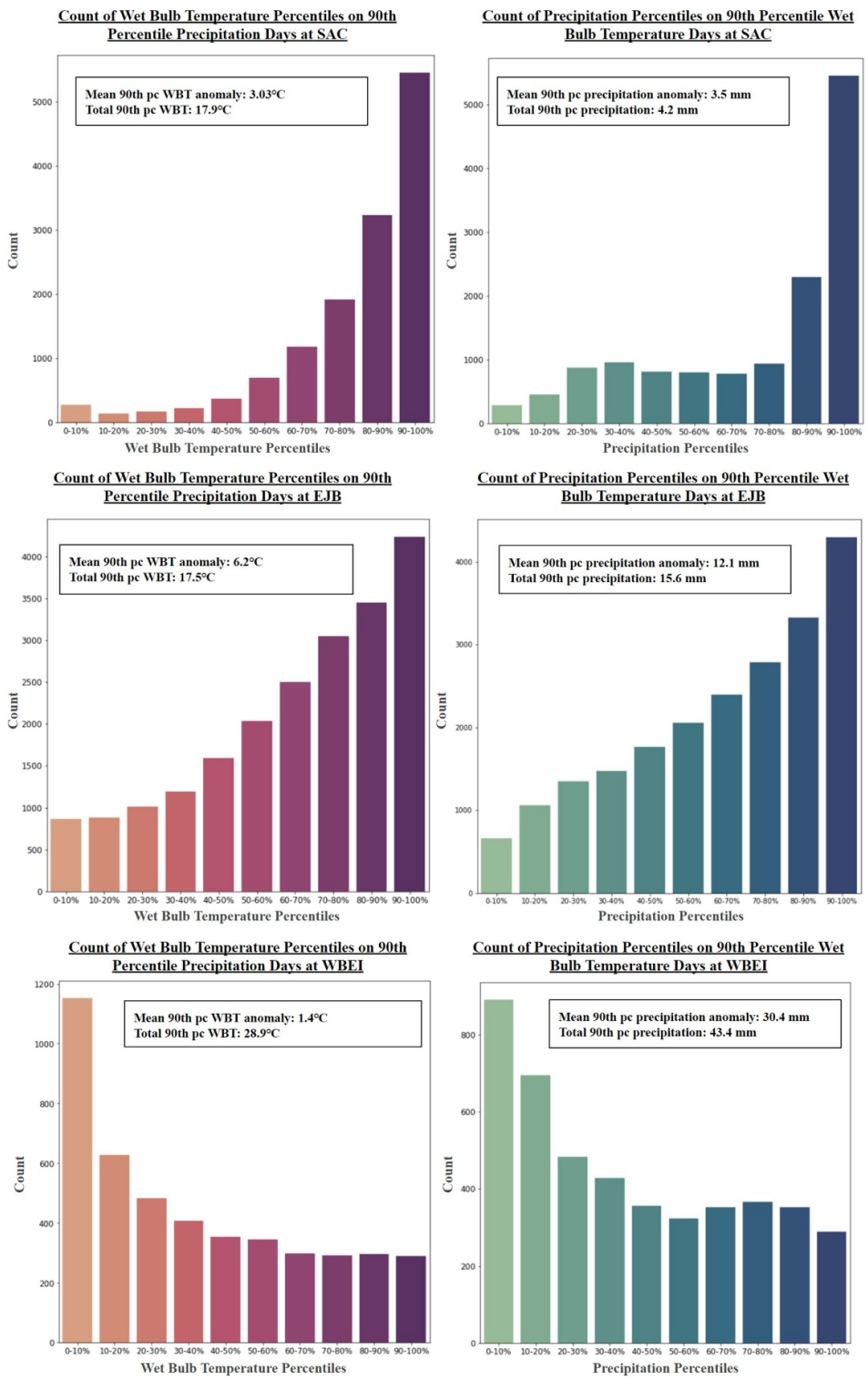

Figure 4. Left column: count of daily maximum wet bulb temperatures within each 10% percentile bin on 90th percentile precipitation days in each subregion. Right column: count of daily total precipitation within each 10% percentile bin on 90th percentile wet bulb temperature days in each subregion.

percentile days for the primary variable (e.g. the distribution of WBT conditioned on 90th percentile precipitation days), using the same three regions. While these results reinforce the findings above, they allow an added assessment of the joint risk of presumably even more societally impactful multivariate 90th percentile extremes in *both* variables. Of note, in SAC approximately 40% of all extreme precipitation

days feature 90th percentile or greater WBTs, pointing to potential multivariate risks that are worthy of further study. In contrast, in WBEI, there is fortunately an outsized preponderance of lowest percentile bins in the secondary variable accompanying 90th percentiles in the primary variable. This points to the possibility of slightly reduced joint risks, although the high baseline values for both variables, and the relatively low variance in WBT, likely partially temper the importance of this result.

4. Discussion and conclusion

We have analyzed globally the temporal relationship between extreme humid heat and rainfall, and between extreme rainfall and humid heat. In select subregions, we have also unpacked how DBT and specific humidity–the two dominant contributors to WBT–evolve along with WBT and precipitation on the days surrounding precipitation extremes. We find lower WBTs on the days after heavy rain for the vast majority of the mid- and high-latitudes, to our knowledge a previously unreported and potentially impactful result. The past decade has seen emerging research about how the latitude, frequency, and magnitude of low pressure systems and associated precipitation in summer might shift northwards and–at least to the south–attenuate in a warming climate. This literature has also pointed to observed increases in DBTs associated with the moisture deficits and other associated factors (e.g. lack of cloud cover and vertical mixing Lehmann and Coumou 2015), accompanying a reduction in the low pressure systems likely to be conducive to 90th percentile precipitation events. But to our knowledge no studies have yet highlighted increases in WBT as a possible result of any reduction in 90th percentile precipitation events, as our findings suggest.

It is similarly noteworthy that in large swathes of the mid-to- high latitudes, the deep tropics and subtropical East Asia, elevated WBTs tend to be preceded by anomalously dry conditions. In contrast, those subtropical regions that tend to be hot, sunny, and lack a consistent moisture source—whether through surface fluxes or via climatological moisture advection–tend to experience extreme WBTs in the presence of and/or immediately following precipitation surpluses. South Asia provides a microcosm of these two regimes. During the June–August season analyzed here, eastern South Asia has abundant moisture sources during monsoon-associated precipitation, associated with the land surface and advection from the adjacent warm Bay of Bengal. In such a moist environment, a period of suppressed precipitation associated with decreased cloud cover and increased sensible heating can allow DBTs to rise without causing the amount of moisture in the air to decrease substantially, intensifying local WBTs (Raymond *et al* 2021, Ivanovich *et al* 2022, 2024). In contrast, western India and Pakistan are climatologically much drier on average and elevated WBTs require an influx of moisture (Monteiro and Caballero 2019). Anomalous precipitation can supply this moisture, leading to positive WBT anomalies which peak the same day as extreme precipitation events. The distinct relationships between WBT and surface moisture fluxes dependent upon land surface characteristics are consistent with recent literature exploring the response of WBT to soil moisture and irrigation (Monteiro and Caballero 2019, Krakauer *et al* 2020, Mishra *et al* 2020, Jha *et al* 2022, Kong and Huber 2023). The possible role of moisture advection in driving up WBTs in these climatologically moisture-limited regions is also worthy of further research, especially since moisture advection, surface moisture fluxes, and their simultaneous and sequential interactions could change in complex and non-linear ways in a warming climate (Rind *et al* 1997).

The Day 0 panels in figures 1 and 2 offer insight about whether extreme precipitation events are more strongly associated with simultaneous WBT or DBT extremes. During times of high potential insolation, under sunny skies surface temperatures can rise substantially, supporting atmospheric instability (Ning *et al* 2022). Nevertheless, figure 1(d) reveals that very few land regions show DBT intensification on the day of extreme precipitation events (Trenberth and Shea 2005). In contrast, figure 1(b) reveals numerous land regions showing positive WBT anomalies on the day of extreme precipitation.

Sub-daily analyses could further illuminate some of these topics. As shown in supplementary figure S6, over a few regions, including much of Eurasia, the transition from anomalously high WBTs to anomalously low actually happens between the day before the anomalous rain and the day of the rain, rather than between Day 0 and Day +1. Similarly, over parts of southeast Asia, precipitation anomalies do not turn positive until the day after the extreme wet bulb event. Midnight as a date marker is somewhat arbitrary; regional variations in time of day of extreme are thus worthy of further study. For example, if a region with a propensity for extreme precipitation in the overnight hours fostered anomalously low WBT maxima later that day, the high precipitation and low WBTs are in some sense not particularly concurrent even though they would register as occurring 'simultaneously' in a daily-resolution analysis. Sub-daily analyses would offer additional benefits by more fully illuminating aspects of extremes such as shorter duration downpours (Fowler *et al* 2021), and the sub-daily distribution of humid heat (Justine *et al* 2023). With respect to the closely related topic of spatial resolution, although supplemental figures S12

and S13 reveal that using observations at 0.5° × 0.5° from NOAA CPC yield very similar results to our 1° × 1° analysis, much higher spatial resolution data products, such as those from remote sensing, would no doubt yield new insights in detailed analyses of regions and events. Indeed, given the fine scale of many precipitation events in most regions, and humid heat in a few select regions, station/point data-based local studies could help illuminate relationships and processes in different microclimatic settings. The results of these subdaily analyses are particularly relevant for evaluating the impacts of compound humid heat-precipitation events, as individuals' behavioral responses to extreme humid heat and precipitation (e.g. seeking shelter or evacuation), may be different if phenomena are occurring at the exact same time or in succession.

At subseasonal scales, positive feedbacks might help explain the existence of select regions, especially in the subtropics, with anomalies of consistent sign before, during, and after a 90th percentile event. For example, in the days leading up to a 90th percentile precipitation event, large-scale circulation might drive positive WBT anomalies, whereas after the rainfall event, evaporation of surface moisture might sustain future positive wet bulb anomalies in a positive feedback. But it is also possible that the long-duration correlation can be better explained by more remote, interannual forcing like ENSO (Speizer *et al* 2022). Even if WBT and precipitation were not mechanistically linked to each other regionally, a tendency for a higher frequency of both events in a certain ENSO phase could as a statistical artifact produce long-duration anomalies of the same sign. More likely, both remote interannual forcing and more local feedbacks can be important in some regions, and can interact (Hendon 2003). At slightly shorter timescales, another question worthy of further research is how the relationships described here vary when sequences of days, each above the 90th percentile occur, as opposed to single day, 'isolated' events (as a global average, isolated events reduce the extreme wet bulb day pool by 21% and the extreme precipitation day pool by 53%). While our proof-of-concept analysis here encompasses both of the above rather than differentiating between the two, supplemental figures S14 and S15 show that for the subset of 'isolated' events the overall patterns are very similar to the main results (where *all* 90th percentile days are composited whether occurring in a sequence of such days, or not), as are the magnitudes when conditioning based on extreme precipitation. When conditioning on WBT, however, the magnitudes are in some locations larger, although the patterns generally remain the same. Analyses that differentiate between isolated 90th percentile and sequential 90th percentile days when looking at the time evolution of the events would no doubt yield additional insights.

Further analyses including model experiments could thus explore whether antecedent precipitation can influence evapotranspiration and surface temperature, and thereby extreme humid heat and extreme precipitation statistics, at time scales longer than the few days assessed here (Wei and Dirmeyer 2019). Additional research could also be devoted to exploring the influence of local precipitation frequency and intensity on the relationships identified here. Future work could explore how the total magnitude of precipitation modulates its influence over humid heat as well as exploring how the length of precipitation events (e.g. one isolated extreme day of intense rainfall versus a particularly strong wet spell during a monsoon season) may influence these relationships. Furthermore, our methodologies could be extended to additional climate variables and thresholds. As an example of the latter, a focus on more rare and societally impactful humid heat and precipitation extremes–such as those that can occasionally form temporary lakes or knock out access to air conditioning or cooling centers–could yield different results. Our analyses in contrast generalize across a large number of relatively moderate (90th percentile or greater; but supplemental figures S10 and S11 show our results are insensitive to using a 95th percentile threshold) extremes, and do not differentiate for example the 99.9th percentile event from the 90th. Because a 90th (or 95th) percentile threshold averages across many types of events, future regional studies could compare for example results from tropical systems to those from frontal systems.

Sequential extremes clearly hold the potential for non-linear impacts, pointing to the need for more impacts and adaptation focused work to expand upon our hazard-based findings described here. As possible examples of future exploratory case studies one can imagine that the positive association between precipitation and humid heat could (1) increase vulnerability during landslides in southern Peru (Millán-Arancibia and Lavado-Casimiro 2023), (2) threaten livestock based livelihoods in the Sahel (due to concurrent animal and human heat stress plus pasture degradation by floods) (Barbier *et al* 2009), and (3) pose challenges for the remote James Bay Cree towns that often feature one access road and one power line (Tam *et al* 2013).

Finally, our work does not explore trends or projections in the humid heat-precipitation relationships described here. The frequency of these event sequences will be influenced by both changes with global warming in the statistical distribution and different spatial patterns of each variable individually, and any changes with warming in the physical mechanisms that connect them (Raymond *et al* 2022). Future concurrence will depend on interactive effects of thermodynamics, dynamics, and land-surface changes, each of

which carries its own uncertainty and modeling challenges.

Data availability statement

Data from ERA5 used in this analysis is publicly accessible via the following website: https://cds.climate.copernicus.eu/cdsapp#!/dataset/reanalysis-era5-single-levels?tab=overview. Other data that support the findings of this study are openly available at the following URL/DOI: https://doi.org/10.24381/cds.adbb2d47. All code used to generate figures is publicly available at the following Github repository: https://github.com/SophKJ/Temporal-connections-between-extreme-precipitation-and-humid-heat.

ORCID iD

Sophie Johnson https://orcid.org/0000-0002-5612-2336

References

Ali H, Fowler H J and Mishra V 2018 Global observational evidence of strong linkage between dew point temperature and precipitation extremes *Geophys. Res. Lett.* **45** 12,320–30

Barbier B, Yacouba H, Karambiri H, Zoromé M and Somé B 2009 Human vulnerability to climate variability in the sahel: farmers' adaptation strategies in Northern Burkina Faso *Environ. Manage.* **43** 790–803

Buzan J R, Oleson K and Huber M 2015 Implementation and comparison of a suite of heat stress metrics within the community land model version 4.5 *Geosci. Model. Dev.* **8** 151–70

Caretta M A *et al* 2022 Water *Climate Change 2022: Impacts, Adaptation and Vulnerability. Contribution of Working Group II to the Sixth Assessment Report of the Intergovernmental Panel on Climate Change* ed H-O Pörtner *et al* (Cambridge University Press) pp 551–712

Chen H and Sun J 2021 Significant increase of the global population exposure to increased precipitation extremes in the future *Earth's Future* **9** e2020EF001941

Chen Y, Liao Z, Shi Y, Tian Y and Zhai P 2021 Detectable increases in sequential flood-heatwave events across China during 1961–2018 *Geophys. Res. Lett.* **48** e2021GL092549

Coffel E D, Horton R M and De Sherbinin A 2017 Temperature and humidity based projections of a rapid rise in global heat stress exposure during the 21st century *Environ. Res. Lett.* **13** 014004

Davies-Jones R 2008 An efficient and accurate method for computing the wet-bulb temperature along pseudoadiabats *Mon. Weather Rev.* **136** 2764–85

Diaz C, Ting M, Horton R, Singh D, Rogers C D W and Coffel E 2023 Increased extreme humid heat hazard faced by agricultural laborers since 1979 *Environ. Res. Commun.* **5** 115013

Easterling D R, Kunkel K E, Arnold J R, Knutson T, LeGrande A N, Leung L R, Vose R S, Waliser D E and Wehner M F 2017 Precipitation change in the United States *Climate Science Special Report: Fourth National Climate Assessment* vol I, ed D J Wuebbles, D W Fahey and K A Hibbard (U.S. Global Change Research Program) (available at: https://pubs.giss.nasa.gov/abs/ea02000c.html)

Fowler H J *et al* 2021 Anthropogenic intensification of short-duration rainfall extremes *Nat. Rev. Earth Environ.* **2** 107–22

Hemmati M, Kornhuber K and Kruczkiewicz A 2022 Enhanced urban adaptation efforts needed to counter rising extreme rainfall risks *npj Urban Sustain.* **2** 16

Hendon H H 2003 Indonesian rainfall variability: impacts of enso and local air–sea interaction *J. Clim.* **16** 1775–90

Hersbach H *et al* 2020 The ERA5 global reanalysis *Q. J. R. Meteorol. Soc.* **146** 1999–2049

Horton R M, Mankin J S, Lesk C, Coffel E and Raymond C 2016 A review of recent advances in research on extreme heat events *Curr. Clim. Change Rep.* **2** 242–59

IPCC 2021 Summary for Policymakers *Climate Change 2021: The Physical Science Basis. Contribution of Working Group I to the Sixth Assessment Report of the Intergovernmental Panel on Climate Change* ed Masson-Delmotte V *et al* accepted

Ivanovich C, Anderson W, Horton R, Raymond C and Sobel A 2022 The influence of intraseasonal oscillations on humid heat in the Persian Gulf and South Asia *J. Clim.* **35** 4309–29

Ivanovich C, Horton R, Sobel A and Singh D 2024 Subseasonal variability of humid heat during the South Asian Summer Monsoon *Geophys. Res. Lett.* **51** e2023GL107382

Jha R, Mondal A, Devanand A, Roxy M K and Ghosh S 2022 Limited influence of irrigation on pre-monsoon heat stress in the Indo-Gangetic plain *Nat. Commun.* **13** 4275

Justine J, Monteiro J M, Shah H and Rao N 2023 The diurnal variation of wet bulb temperatures and exceedance of physiological thresholds relevant to human health in South Asia *Commun. Earth Environ.* **4** 1–11

Kong Q and Huber M 2023 Regimes of soil moisture-wet bulb temperature coupling with relevance to moist heat stress *J. Clim.* **36** 1–45

Kopp B 2020 *WetBulb.m* (available at: https://github.com/bobkopp/WetBulb.m)

Krakauer N Y, Cook B I and Puma M J 2020 Effect of irrigation on humid heat extremes *Environ. Res. Lett.* **15** 094010

Lehmann J and Coumou D 2015 The influence of mid-latitude storm tracks on hot, cold, dry and wet extremes *Sci. Rep.* **5** 17491

Lenderink G and Attema J 2015 A simple scaling approach to produce climate scenarios of local precipitation extremes for the Netherlands *Environ. Res. Lett.* **10** 085001

Matthews T, Wilby R L and Murphy C 2019 An emerging tropical cyclone–deadly heat compound hazard *Nat. Clim. Change* **9** 602–6

Millán-Arancibia C and Lavado-Casimiro W 2023 Rainfall thresholds estimation for shallow landslides in Peru from gridded daily data *Nat. Hazards Earth Syst. Sci.* **23** 1191–206

Mishra V, Ambika A K, Asoka A, Aadhar S, Buzan J, Kumar R and Huber M 2020 Moist heat stress extremes in India enhanced by irrigation *Nat. Geosci.* **13** 722–8

Monteiro J M and Caballero R 2019 Characterization of extreme wet-bulb temperature events in Southern Pakistan *Geophys. Res. Lett.* **46** 10659–68

Ning G, Luo M, Zhang W, Liu Z, Wang S and Gao T 2022 Rising risks of compound extreme heat-precipitation events in China *Int. J. Climatol.* **42** 5785–95

Prein A, Rasmussen R, Ikeda K, Liu C, Clark M P and Holland G J 2017 The future intensification of hourly precipitation extremes *Nat. Clim. Change* **7** 48–52

Raymond C, Matthews T and Horton R M 2020 The emergence of heat and humidity too severe for human tolerance *Sci. Adv.* **6** eaaw1838

Raymond C, Matthews T, Horton R M, Fischer E M, Fueglistaler S, Ivanovich C, Suarez-Gutierrez L and Zhang Y 2021 On the controlling factors for globally extreme humid heat *Geophys. Res. Lett.* **48** e2021GL096082

Raymond C, Suarez-Gutierrez L, Kornhuber K, Pascolini-Campbell M, Sillmann J and Waliser D E 2022 Increasing spatiotemporal proximity of heat and precipitation extremes in a warming world quantified by a large model ensemble *Environ. Res. Lett.* **17** 035005

Rind D, Rosenzweig C and Stieglitz M 1997 The role of moisture transport between ground and atmosphere in global change *Annu. Rev. Energy Environ.* **22** 47–74

Robinson A *et al* 2021 Increasing heat and rainfall extremes now far outside the historical climate *npj Clim. Atmos. Sci.* **4** 45

Rogers C D, Ting M, Li C, Kornhuber K, Coffel E D, Horton R M and Singh D 2021 Recent increases in exposure to extreme humid-heat events disproportionately affect populated regions *Geophys. Res. Lett.* **48** e2021GL094183

Romanello M, Di Napoli C, Drummond P, Green C, Kennard H, Lampard P and Costello A 2022 The 2022 report of the Lancet Countdown on health and climate change: health at the mercy of fossil fuels *Lancet* **400** 1619–54

Sherwood S C and Huber M 2010 An adaptability limit to climate change due to heat stress *Proc. Natl Acad. Sci.* **107** 9552–5

Speizer S, Raymond C, Ivanovich C and Horton R M 2022 Concentrated and intensifying humid heat extremes in the IPCC AR6 regions *Geophys. Res. Lett.* **49** e2021GL097261

Sun Q, Zhang X, Zwiers F, Westra S and Alexander L V 2021 A global, continental, and regional analysis of changes in extreme precipitation *J. Clim.* **34** 243–58

Tam B Y, Gough W A, Edwards V and Tsuji L J S 2013 The impact of climate change on the well-being and lifestyle of a First Nation community in the western James Bay region *Can. Geogr./Géogr. Can.* **57** 441–56

Trenberth K E and Shea D J 2005 Relationships between precipitation and surface temperature *Geophys. Res. Lett.* **32** 2005GL022760

Wei J and Dirmeyer P A 2019 Sensitivity of land precipitation to surface evapotranspiration: a nonlocal perspective based on water vapor transport *Geophys. Res. Lett.* **46** 12588–97

Wu G and Wang K 2021 Observed response of precipitation intensity to dew point temperature over the contiguous US *Theor Appl. Climatol.* **144** 1349–62

Zhang W and Villarini G 2020 Deadly compound heat stress-flooding hazard across the Central United States *Geophys. Res. Lett.* **47** e2020GL089185

Zhang X, Zwiers F W, Li G, Wan H and Cannon A J 2017 Complexity in estimating past and future extreme short-duration rainfall *Nat. Geosci.* **10** 255–9

Zscheischler J *et al* 2020 A typology of compound weather and climate events *Nat. Rev. Earth Environ.* **1** 333–47